Neglecting the switching ripple

Suppose the duty cycle is modulated sinusoidally:

$$d(t) = D + D_m \cos \omega_m t$$

where D and D_m are constants, $|D_m| \ll D$, and the modulation frequency ω_m is much smaller than the converter switching frequency $\omega_s = 2\pi f_s$.

The resulting variations in transistor gate drive signal and converter output voltage:

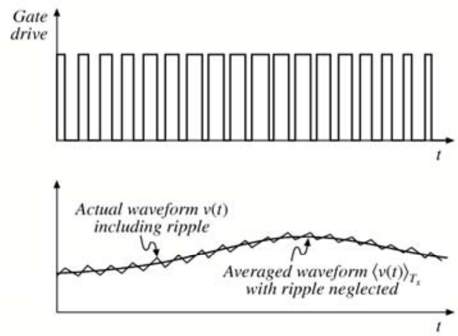

Output voltage spectrum
with sinusoidal modulation of duty cycle

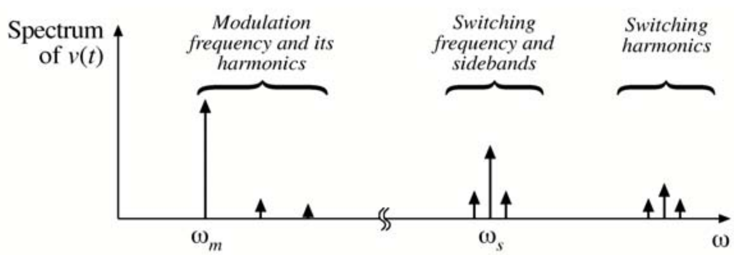

Contains frequency components at:

- Modulation frequency and its harmonics
- Switching frequency and its harmonics
- Sidebands of switching frequency

With small switching ripple, high-frequency components (switching harmonics and sidebands) are small.

If ripple is neglected, then only low-frequency components (modulation frequency and harmonics) remain.

Sampling

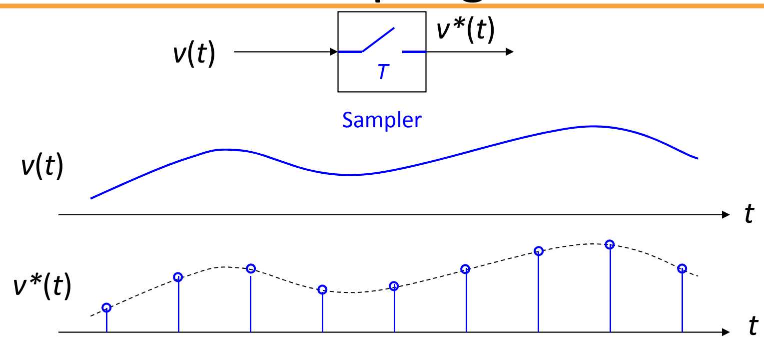

$$v^*(t) = v(t)\sum_{-\infty}^{+\infty}\delta(t - nT)$$

Unit impulse (Dirac)

Sampled-data system example: frequency domain

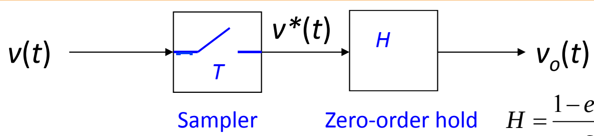

$$H = \frac{1 - e^{-sT}}{s}$$

$$v^*(s) = \frac{1}{T}\sum_{k=-\infty}^{+\infty} v(s - jk\omega_s)$$

$$v_o(s) = \frac{1 - e^{-sT}}{s} v^*(s) = \frac{1 - e^{-sT}}{sT}\sum_{k=-\infty}^{+\infty} v(s - jk\omega_s)$$

Consider only low-frequency signals: $v_o(s) \approx \frac{1 - e^{-sT}}{sT} v(s)$

System “transfer function” = $\frac{v_o}{v} = \frac{1 - e^{-sT}}{sT}$

Zero-order hold: frequency responses

f_s = 1 MHz

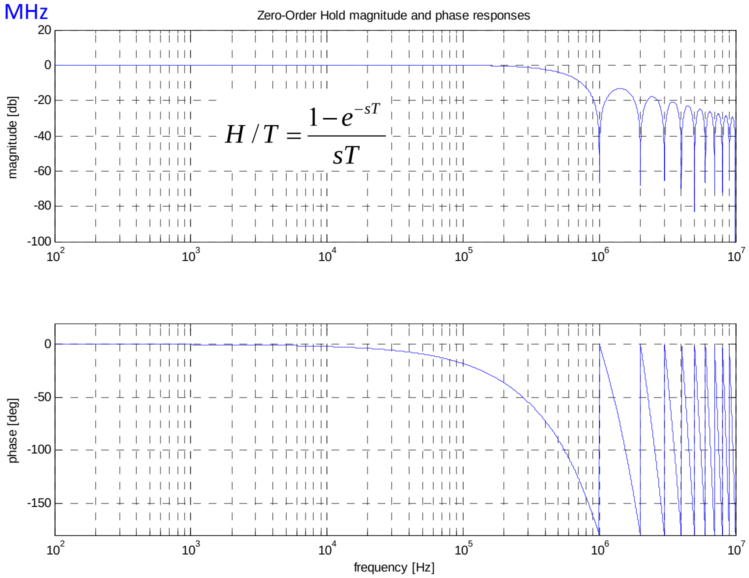

How does any of this apply to converter modeling?

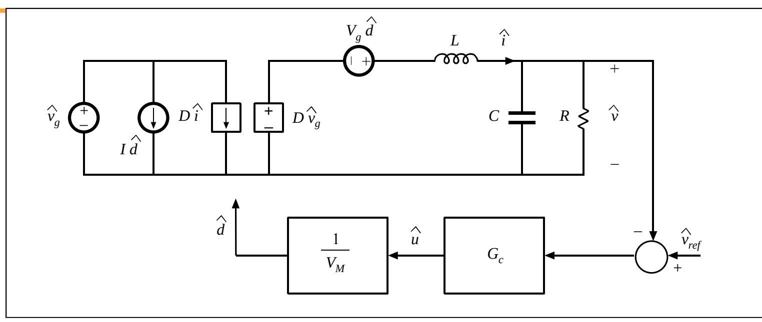

PWM is a small-signal sampler!

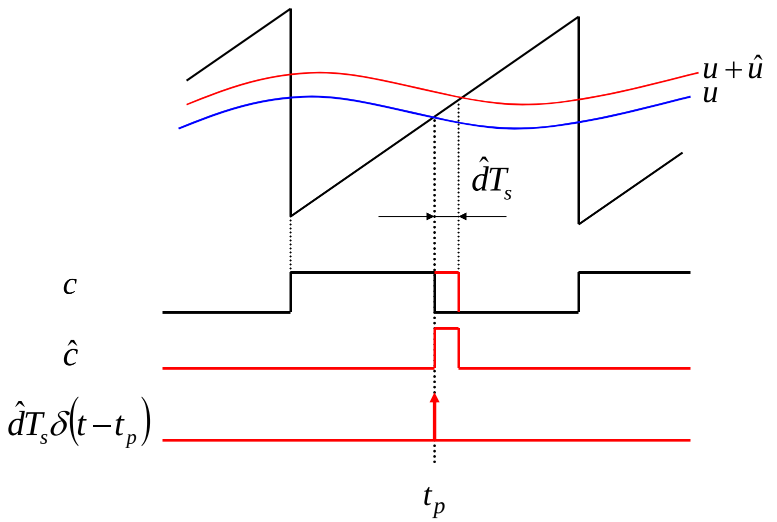

PWM sampling occurs at t_p (*i.e.* at dT_s, periodically, in each switching period)

General sampled-data model

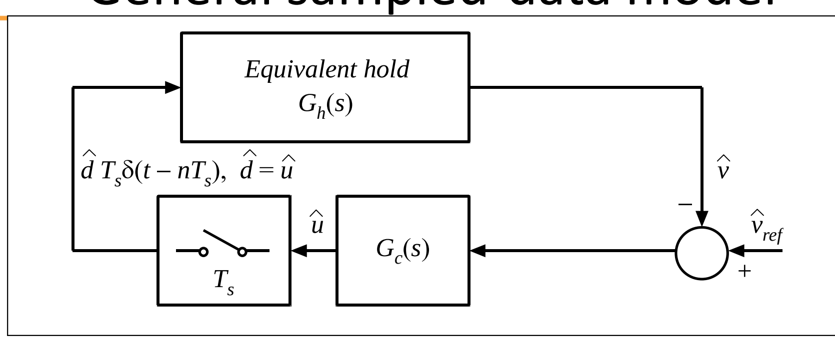

- Sampled-data model valid at all frequencies
- *Equivalent hold* describes the converter small-signal response to the sampled duty-cycle perturbations [Billy Lau, PESC 1986]
- State-space averaging or averaged-switch models are low-frequency continuous-time approximations to this sampled-data model

Application to DCM high-frequency modeling

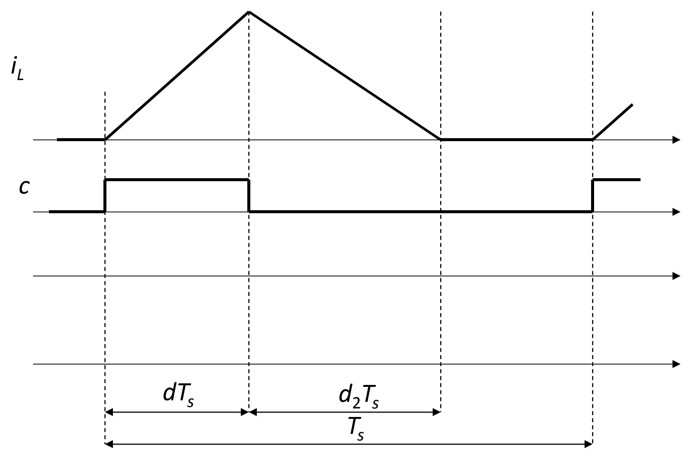

Application to DCM high-frequency modeling

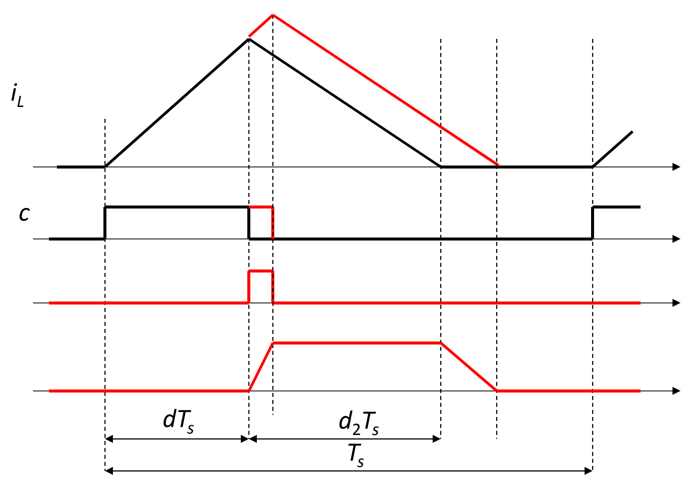

DCM inductor current high-frequency response

$$\hat{i}_L(s) = \frac{V_1+V_2}{L} T_s \frac{1-e^{-sD_2T_s}}{s} \hat{d}^*(s) = \frac{V_1+V_2}{L} T_s \frac{1-e^{-sD_2T_s}}{s} \frac{1}{T_s} \sum_{k=-\infty}^{+\infty} \hat{d}(s - jk\omega_s)$$

$$\hat{i}_L(s) \approx \frac{V_1+V_2}{L} D_2T_s \frac{1-e^{-sD_2T_s}}{D_2T_s s} \hat{d}(s)$$

$$\frac{\hat{i}_L(s)}{\hat{d}(s)} \approx \frac{V_1+V_2}{L} D_2T_s \frac{1}{1+\dfrac{s}{\omega_2}} \qquad \omega_2 = \frac{2}{D_2T_s}$$

$$f_2 = \frac{f_s}{\pi D_2}$$

High-frequency pole due to the inductor current dynamics in DCM, see (11.77) in Section 11.3

Example DAB Application

- Goal: Include effects of both output sampling and PWM sampling in converter model
- Considering only control perturbations, model will take the form

$$\hat{x}[n] = F\hat{x}[n-1] + G\hat{\varphi}_{ab}[n-1]$$

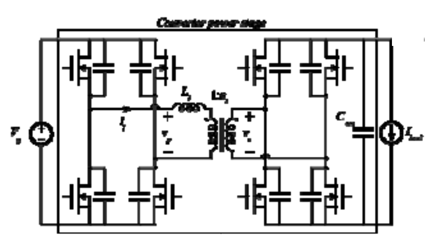

Example DAB Application

- Goal is to develop a model of the form

$$\hat{x}[n] = F\hat{x}[n-1] + G\hat{\varphi}_{ab}[n-1]$$

- State vector is sampled and control updated at $t=nT_s$

$$x = \begin{bmatrix} v_p & i_l & v_{out} \end{bmatrix}^T$$

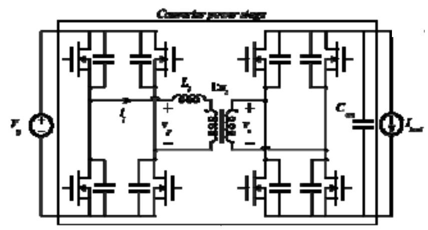

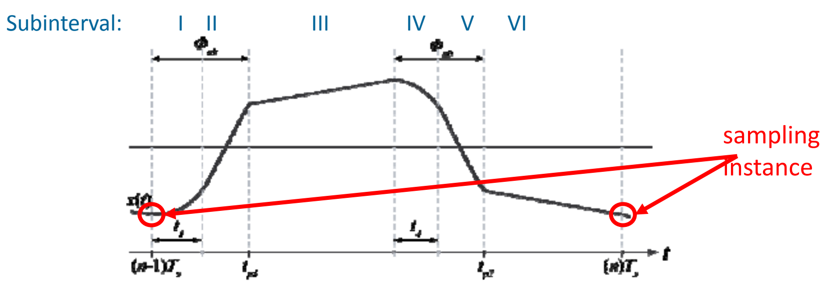

Continuous Time State Space

$$\dot{x}(t) = A_i x(t) + B_i V_g$$

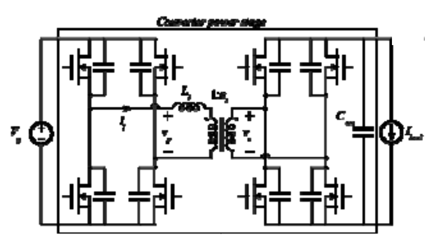

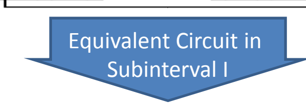

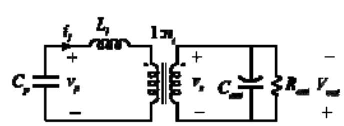

Continuous Time State Representation

$$\dot{x}(t) = A_i x(t) + B_i V_g$$

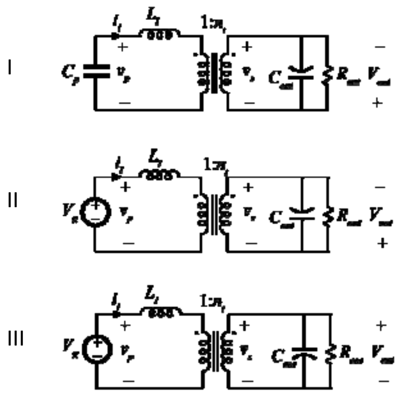

$$A_1 = \begin{bmatrix} 0 & 0 & \frac{-1}{C_p} \\ 0 & \frac{-1}{C_{out}R_{out}} & \frac{1}{C_{out}n_t} \\ \frac{1}{L_l} & \frac{-1}{L_l n_t} & 0 \end{bmatrix} \quad B_1 = \begin{bmatrix} 0 \\ 0 \\ 0 \end{bmatrix}$$

$$A_2 = \begin{bmatrix} \frac{-1}{2R_pC_p} & 0 & 0 \\ 0 & \frac{-1}{C_{out}R_{out}} & \frac{1}{C_{out}n_t} \\ 0 & \frac{-1}{L_l n_t} & 0 \end{bmatrix} \quad B_2 = \begin{bmatrix} \frac{-1}{2R_pC_p} \\ 0 \\ \frac{-1}{L_l} \end{bmatrix}$$

$$A_3 = \begin{bmatrix} \frac{-1}{2R_pC_p} & 0 & 0 \\ 0 & \frac{-1}{C_{out}R_{out}} & \frac{-1}{C_{out}n_t} \\ 0 & \frac{1}{L_l n_t} & 0 \end{bmatrix} \quad B_3 = \begin{bmatrix} \frac{-1}{2R_pC_p} \\ 0 \\ \frac{-1}{L_l} \end{bmatrix}$$

- Models change slightly depending on operating mode
- In all cases, consider dynamics at boundary just below ZVS

State Propagation

- Within each subinterval, states propagate according to continuous time model

$$\dot{x}(t) = A_i x(t) + B_i V_g$$

- Solution given by

$$x(t) = e^{A_i t} x_0 + \int_0^{t_i} e^{-A_i(t-\tau)} \left(B_i v_g(\tau)\right) d\tau \ .$$

- If $v_g(t) \approx V_g$ within one switching period,

$$x_1(t_1) = e^{A_1 t_1} x_0 + A_1^{-1}\left(e^{A_1 t_1} - I\right) B_1 V_g$$

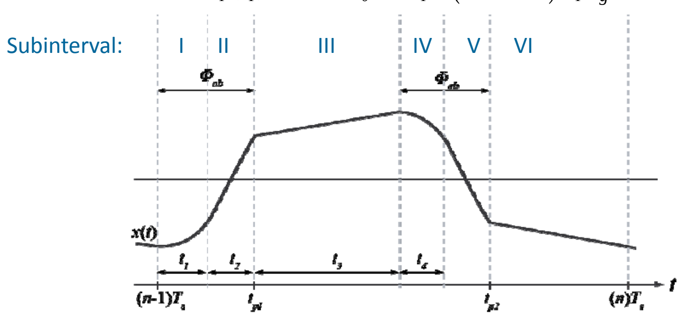

Small Signal State Propagation

- Considering steady state plus some small signal, solution becomes

$$X_1 + \hat{x}_1 = e^{A_1 t_1}\left(X_0 + \hat{x}_0\right) + A_1^{-1}\left(e^{A_1 t_1} - I\right)B_1 V_g$$

- Small signal portion can be separated out

$$\hat{x}_1 = e^{A_1 t_1}\hat{x}_0$$

- And applied for each subinterval to obtain natural response

$$F = e^{A_6 t_6} e^{A_5 t_5} e^{A_4 t_4} e^{A_3 t_3} e^{A_2 t_2} e^{A_1 t_1}$$

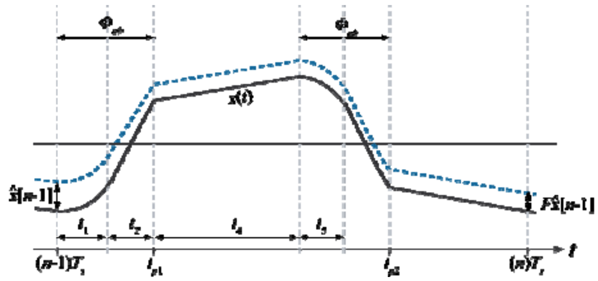

Small Signal Response to Phase Perturbation

- For the forced response, consider the effect of an increase in phase shift interval of magnitude $\hat{\varphi}_{ab}$ around steady-state vector X_{p1}

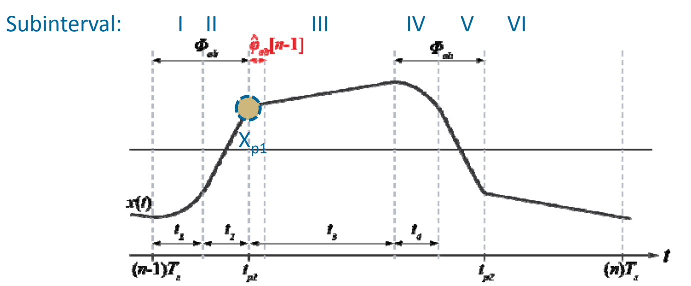

Small Signal Response to Phase Perturbation

- Perturbation in phase shift $\hat{\varphi}_{ab}$ results in a state perturbation $\hat{x}_{d1}$
- In accordance with small signal modeling assumptions, affect on phase perturbations on state assumed to be instantaneous

$$\hat{x}_{d1} = (A_2 - A_3) X_{p1} \frac{T_s}{2\pi} \hat{\varphi}_{ab}$$

Subinterval: I II IV V VI VIII

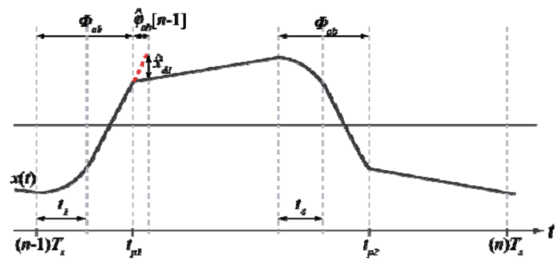

Small Signal Response to Phase Perturbation

- Perturbation in phase shift $\hat{\varphi}_{ab}$ results in a state perturbation $\hat{x}_{d1}$
- In accordance with small signal modeling assumptions, affect on phase perturbations on state assumed to be instantaneous
- State perturbation is then similarly propagated through state progression to next sampling interval

$$\chi_1 \hat{x}_{d1} = e^{A_6 t_6} e^{A_5 t_5} e^{A_4 t_4} (A_2 - A_3) X_{p1} \frac{T_s}{2\pi} \hat{\varphi}_{ab}$$

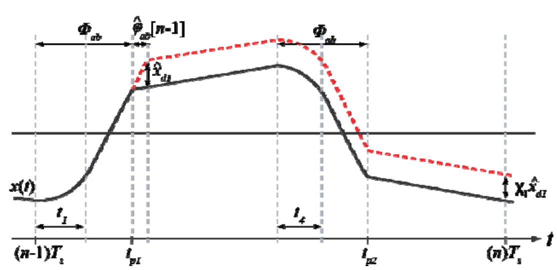

Small Signal Response to Phase Perturbation

- Perturbation in phase shift $\hat{\varphi}_{ab}$ results in a state perturbation $\hat{x}_{d1}$
- In accordance with small signal modeling assumptions, affect on phase perturbations on state assumed to be instantaneous
- Perturbations propagated to output for two independent changes in state at next sampling instant

$$G = e^{A_6 t_6} e^{A_5 t_5} e^{A_4 t_4} \left(A_2 - A_3\right) X_{p1} \frac{T_s}{2\pi} + e^{A_6 t_6} \left(A_5 - A_6\right) X_{p2} \frac{T_s}{2\pi}$$

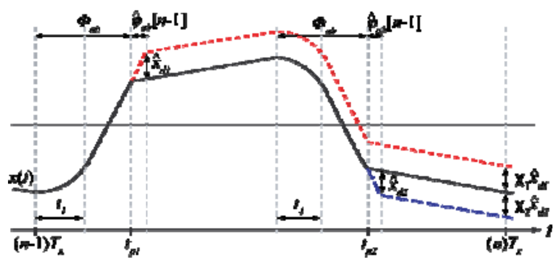

Complete Discrete Time Model

- Combining forced and natural responses into
- Full model is obtained

$$\hat{x}[n] = F\hat{x}[n-1] + G\hat{\varphi}_{ab}[n-1]$$

$$\hat{x}[n] = \left(e^{A_6 t_6} e^{A_5 t_5} e^{A_4 t_4} e^{A_3 t_3} e^{A_2 t_2} e^{A_1 t_1}\right)\hat{x}[n-1] + \ldots$$

$$\left(e^{A_6 t_6} e^{A_5 t_5} e^{A_4 t_4} \left(A_2 - A_3\right) X_{p1} \frac{T_s}{2\pi} + e^{A_6 t_6} \left(A_5 - A_6\right) X_{p2} \frac{T_s}{2\pi}\right)\hat{\varphi}_{ab}$$

- Model can be further simplified through recognition of half-cycle symmetry

Half-Cycle Symmetry

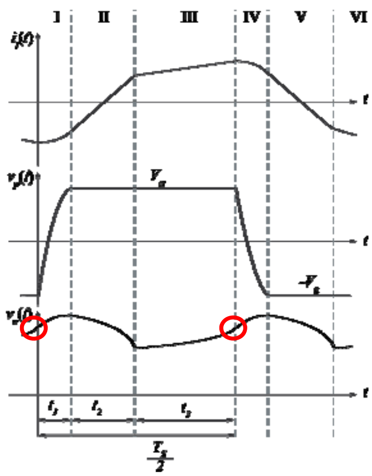

- All states are either symmetric or antisymmetric about the half-period
- Can sample and control at twice the switching frequency:

$$x\left(t+\frac{T_s}{2}\right)=\mathrm{I}_{HC}\,x(t)$$

$$\mathrm{I}_{HC}=\begin{bmatrix}-1 & 0 & 0\\ 0 & -1 & 0\\ 0 & 0 & 1\end{bmatrix}$$

$$\hat{x}[n]=\left(e^{A_3t_3}e^{A_2t_2}e^{A_1t_1}I_{HC}\right)\hat{x}[n-1]+\left(e^{A_3t_3}\left(A_2-A_3\right)X_{p1}\frac{T_s}{2\pi}\right)\hat{\varphi}_{ab}[n-1]$$

DAB: Experimental Results

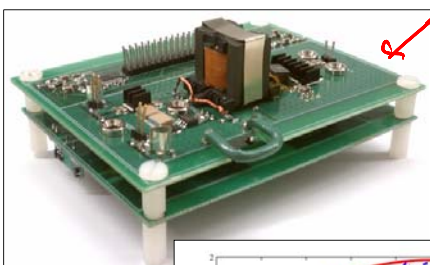

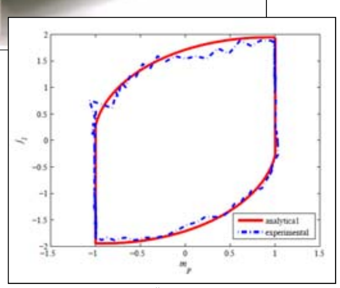

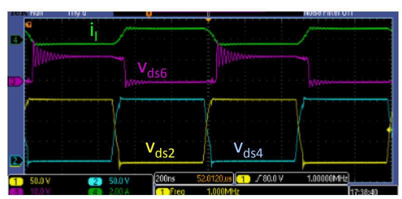

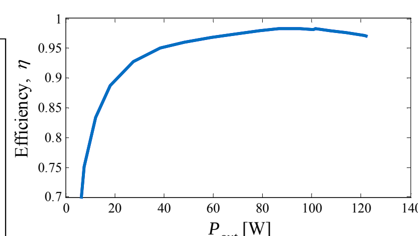

D. Costinett, H. Nguyen, R. Zane, and D. Maksimovic, "GaN-FET based dual active bridge DC-DC converter," in Proc. Appl. Power Electron. Conf. (APEC), march 2011, pp. 1425 –1432.

D. Costinett, D. Maksimovic, and R. Zane, "Design and control for high efficiency in high step-down dual active bridge converters operating at high switching frequency," IEEE Trans. Power Electron., vol. PP, no. 99, p. 1, 2012.

Frequency Response Comparison

P_{out} = 30 W | P_{out} = 90 W

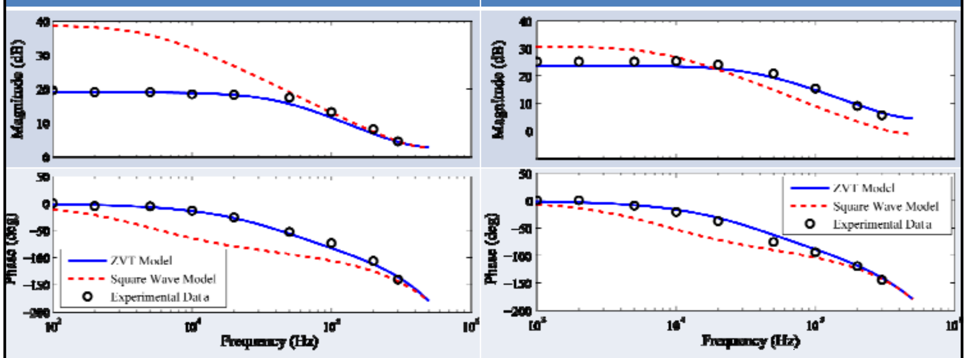

- Bode plot compared to traditional averaged model (neglects ZVS dynamics
- Experimental results verify very little change in dynamics other than DC gain

Transient Response Comparison

P_{out} = 30 W | P_{out} = 90 W

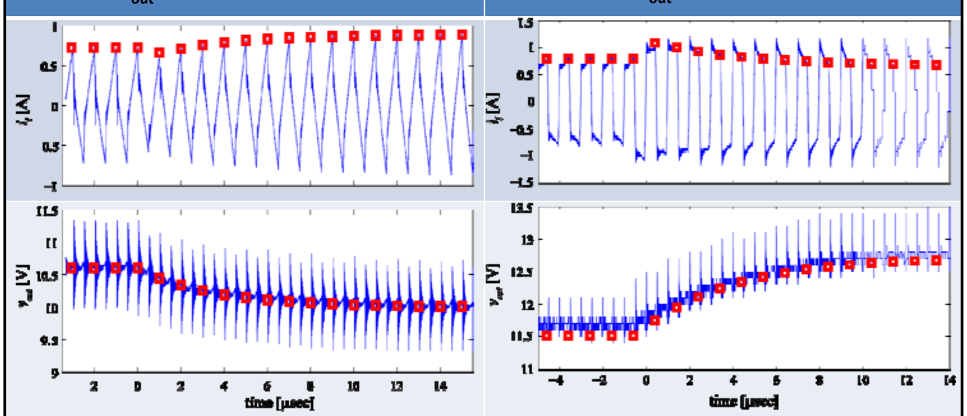

- Response in current and voltage shown at 30 W (left) and 90 W (right) for step changes in φ_{ab}
- Both well matched to experimental results

Additional Readings

[1] D. J. Packard, “Discrete modeling and analysis of switching regulators,” Ph.D. dissertation, California Institute of Technology, Nov. 1976.

[2] A. R. Brown and R. D. Middlebrook, “Sampled-data modeling of switching regulators,” p. 349 369, 1984.

[3] D. Maksimovic and R. Zane, “Small-signal discrete-time modeling of digitally controlled PWM converters,” IEEE Trans. Power Electron., vol. 22, no. 6, pp. 2552 –2556, nov. 2007.

Power Electronics Courses at UTK

Junior

ECE 325
Electric Energy System Components

Senior

ECE 481
Power Electronics

ECE 482 / 599
Power Electronic Circuits

Graduate

ECE 523
Power Electronics and Drives

ECE 623
Advanced Power Electronics and Drives

ECE 625
Utility Applications of Power Electronics

ECE 525
Alternative Energy Sources

ECE 626
Solid State Power Semiconductors

ECE 581
High Frequency Power Electronics

ECE 691/2
Advanced Graduate Seminar 2